

# PROCEEDINGS OF SPIE

[SPIDigitalLibrary.org/conference-proceedings-of-spie](https://spiedigitallibrary.org/conference-proceedings-of-spie)

## Coherent 24 GHz FMCW radar system for micro-Doppler studies

Samiur Rahman, Duncan A. Robertson

Samiur Rahman, Duncan A. Robertson, "Coherent 24 GHz FMCW radar system for micro-Doppler studies," Proc. SPIE 10633, Radar Sensor Technology XXII, 106330I (4 May 2018); doi: 10.1117/12.2304368

**SPIE.**

Event: SPIE Defense + Security, 2018, Orlando, Florida, United States

# Coherent 24 GHz FMCW radar system for micro-Doppler studies

Samiur Rahman<sup>a</sup>, Duncan A. Robertson<sup>a</sup>

<sup>a</sup> University of St Andrews, SUPA School of Physics & Astronomy, St Andrews, Fife KY16 9SS, Scotland

## ABSTRACT

This paper presents the hardware design of a coherent 24 GHz radar system developed at the University of St Andrews to obtain micro-Doppler data. The system is based on the Analog Devices EV-RADAR-MMIC2 evaluation board which is based around a chipset of three integrated circuits: a two channel transmitter, a four channel receiver and a fractional-N frequency synthesizer. The evaluation board is combined with a number of other components to enable coherent operation with a PC-based data acquisition card and to boost the output power to increase the operational range. Three identical custom-made smooth-walled conical horn antennas for transmit and co- and cross-polar receive signals were designed and built for the radar system. It is shown that the performance of these high gain (24.5 dBi) antennas agrees extremely well with the design simulations. Finally, field trial results comprising human, bird and drone micro-Doppler data are shown to validate the system performance.

**Keywords:** Micro-Doppler, Radar, K-band, FMCW

## 1. INTRODUCTION

Micro-Doppler is an intrinsic feature of many targets of interest (i.e. humans, birds, rotary wing UAVs)<sup>1,2</sup>. A surveillance radar system can use this characteristic to identify the object. Target discrimination is also possible as different targets will produce different micro-Doppler signatures unique to their micro-motion properties. A radar sensor capable of extracting targets' micro-Doppler signature can be used widely in both military and civilian applications.

Based on the mathematical groundwork of the radar micro-Doppler phenomenon<sup>3</sup>, a plethora of research works have been conducted, predominantly at frequencies up to X-band<sup>4,5,6,7,8,9</sup>. Most of the purpose built coherent radar systems that are commercially available usually operate from L-band to X-band. However, in general, higher frequency radar systems are able to capture a larger micro-Doppler spread, which has been demonstrated with millimeter wave radars in various research works<sup>10,11,12,13</sup>. For targets like drones which have very fast rotating propellers, higher frequency signals will produce better micro-Doppler signatures with better Doppler resolution, given appropriate sampling. On the other hand, range coverage will tend to become reduced with increasing frequency. As a trade-off, a 24 GHz radar system can provide satisfactory micro-Doppler signature collection with adequate range coverage. Along with drones, this can be useful to obtain micro-Doppler signatures of other targets. Additionally, a key attraction of operating at 24 GHz is the availability of highly integrated radar chipsets, principally developed for the automotive market, which offer a potentially low cost solution.

In this paper, we will discuss the hardware design of a coherent 24 GHz radar system developed at the University of St Andrews for obtaining micro-Doppler data. Exploiting the use of low-cost K-band components, the goal was to build an affordable and reasonably compact data collection radar with sufficient performance to be able to gather high fidelity micro-Doppler signatures of a variety of targets at ranges relevant for surveillance applications. To achieve this, we enhanced the functionality of the radar chipset evaluation board by adding (i) external components to enable coherent operation with PC-based data acquisition card, (ii) a power amplifier to extend the operating range, and (iii) high gain horn antennas to provide sufficient directionality and increase signal-to-noise ratio (SNR). The hardware architecture is presented in section 2 and details of the horn antennas are given in section 3. We have successfully used the radar to collect data on a variety of targets including humans, birds and drones. Results illustrating the micro-Doppler signatures of all these targets are shown in the section 4, validating the system performance.

\*<mailto:sr206@st-andrews.ac.uk>; phone +44 1334 463155; [www.st-andrews.ac.uk/~mmwave](http://www.st-andrews.ac.uk/~mmwave)

Radar Sensor Technology XXII, edited by Kenneth I. Ranney, Armin Doerry,  
Proc. of SPIE Vol. 10633, 1063301 · © 2018 SPIE · CCC code: 0277-786X/18/\$18  
doi: 10.1117/12.2304368

Proc. of SPIE Vol. 10633 1063301-1

## 2. 24 GHZ RADAR ARCHITECTURE

A block diagram of the whole radar is shown in Fig. 1. The following subsections describe the 24 GHz radar chipset evaluation board, the additional components for coherent, longer range operation, and the horn antennas.

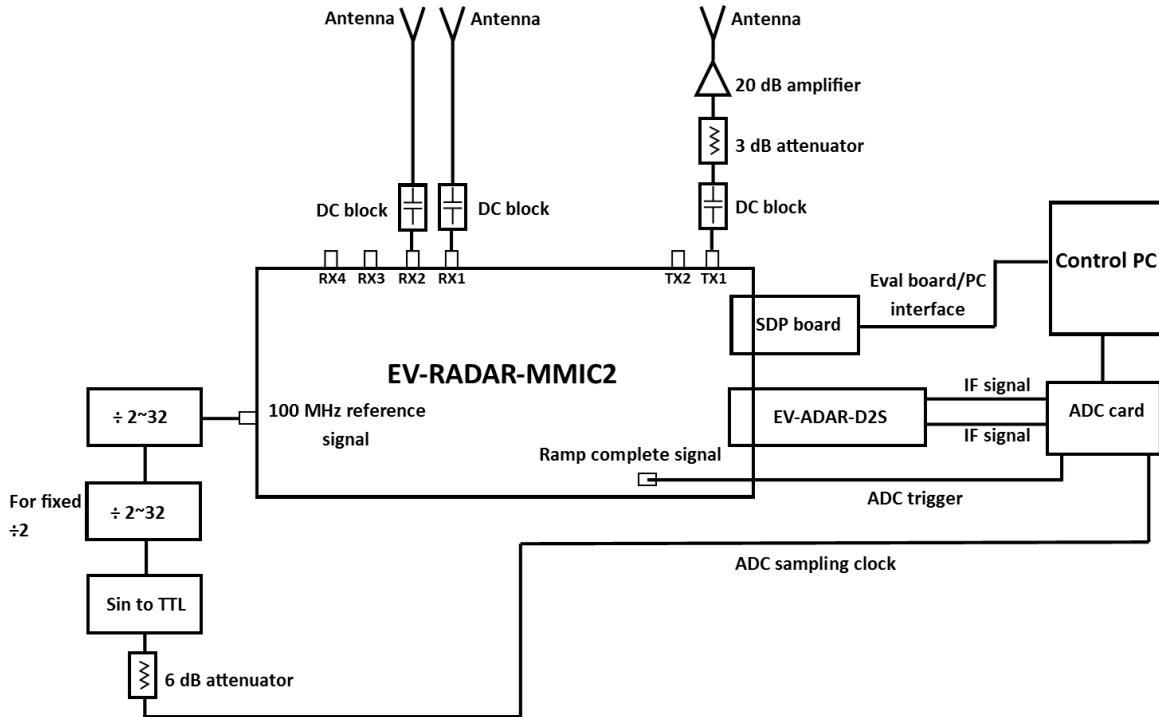


Figure 1. Block diagram of the coherent 24 GHz radar architecture

### 2.1 Analog Devices radar evaluation board

The evaluation board is the Analog Devices EV-RADAR-MMIC2<sup>14</sup>, which enables the user to evaluate the performance of a radar chipset comprising a two channel transmitter chip (ADF5901), a four channel receiver chip (ADF5904) and a fractional-N synthesizer chip (ADF4159) for Frequency Modulated Continuous Wave (FMCW) operation. The evaluation board comes with the EV-ADAR-D2S baseband adapter board which physically attaches to the main evaluation board. This converts the ADF5904 differential baseband signals to single-ended signals. The evaluation board is controlled from a PC over USB via a microcontroller interface board (SDP-B) which also physically attaches to the main board. Evaluation software provided by the manufacturer provides a user interface from which one can control all the functions of all three chips such as transmit or receive channel enable, FMCW chirp duration and bandwidth etc. The various boards can be seen in Fig. 1.

The ADF5901 monolithic microwave integrated circuit (MMIC) transmitter is based around an on-chip 24 GHz voltage controlled oscillator (VCO) with dual buffered transmit channel outputs. The chip also provides a copy of the VCO output as the local oscillator (LO) signal for the receiver chip to enable homodyne FMCW operation and an output at half the VCO frequency to enable frequency control with the PLL chip. The maximum transmitter output from a single channel is +8 dBm and the maximum signal bandwidth that can be achieved is 250 MHz.

The ADF5904 receiver is a 24 GHz MMIC with four identical channels. Each channel includes a single-ended RF input with an on-chip balun, a differential low noise amplifier (LNA), a downconverter mixer and a differential output amplifier. The total receiver channel gain is 22 dB and the noise figure is 10 dB. The differential baseband signals from the ADF5904 are converted to single-ended signals by the EV-ADAR-D2S board which has an additional gain of 20 dB per channel.

Frequency modulation is performed by the ADF4159 which is a 13 GHz fractional-N frequency synthesizer, incorporating a low noise phase frequency detector (PFD). The half frequency output of the VCO at ~12 GHz is used as the synthesizer input signal. The maximum PFD frequency during operation can be 110 MHz. The main board includes a 100 MHz crystal oscillator which provides the reference frequency for the synthesizer. The ADF4159 can generate five different waveforms but for this particular radar configuration, continuous sawtooth ramping was used. The desired ramp setting is attained by adjusting three factors by writing register values: frequency deviation, timeout interval and number of steps. The frequency deviation is set by the PFD frequency, a 16 bit word, and two 4 bit word values (named *DEV* and *DEV\_OFFSET* respectively). The time between each frequency hop (timeout interval) is set by using two 12 bit clock values (named *CLK1* and *CLK2*), along with the PFD frequency. Finally, a 20 bit step value in a register is used to determine the number of steps. Further details of the operation of all these chips can be found in their corresponding datasheets<sup>14</sup>.

## 2.2 Modifications for coherent longer range operation

To make the radar coherent with a PC-based data acquisition card, the ADC sampling and the chirp timing need to be synchronized. For the ADC, a 16-bit, 4 channel, 40 MS/s, ADLINK 9846D PCI card was available which has the option to use external sampling clock and trigger signals. As seen in Fig. 1, the evaluation board has an output port, from which the internal 100 MHz reference signal can be accessed. The sampling clock signal is obtained by dividing the reference clock. Two 5-bit frequency dividers (Analog Devices HMC394LP4 evaluation boards) are used to obtain the desired sampling rate. The first divider can be set to any value between 2 and 32 but the output has an asymmetric duty cycle for values >2 so a second divider which is fixed at  $\div 2$  is used to maintain a 50-50 duty cycle. Finally, a Sin to TTL circuit interfaces to the external clock input of the ADC card. The range of sampling rates available from this frequency division chain is 1.5625 MS/s to 25 MS/s which is consistent with the maximum sampling rate the ADC of 40 MS/s.

The ADC needs to be triggered by an external signal which is synchronized to the chirp repetition frequency. The evaluation board has a test pin which can be configured to generate a pulse after each ramp completion. The falling edge of this pulse corresponds to the start of the next chirp, hence this is used to trigger the ADC to start the sampling. As the 100 MHz signal is the main reference input for the ADF4159 operation, the trigger and the sampling clock signals will be aligned, ensuring the coherence. Along with the evaluation board software, the radar operation is controlled by a user interface written in C using the National Instruments LabWindows/CVI programming environment. Typical data settings in the code allow for acquiring 512 samples per chirp and 128 chirps per burst (coherent processing interval, CPI), which makes 65,536 samples in total. These consecutive 128 chirps are used to generate a single range-Doppler profile. The program allows for continuous acquisition, providing live updates while the radar is in operation. It also has the option for saving data (both in time and frequency domains) for post processing.

To increase the range coverage, a K-band power amplifier is connected between the transmit port and the transmit antenna. The amplifier is a commercially available module based on the Analog Devices HMC863LP4 GaAs pHEMT MMIC. As the amplifier reaches its 1 dB compression point when the input is more than +5 dBm and the transmitter output is +8 dBm, a 3 dB attenuator is connected to the amplifier input. This gives the radar a transmit power of +25 dBm.

The whole 24 GHz radar system is shown in Fig. 2. Note that two receive channels are used to collect co-polar and cross-polar signals. The antennas are discussed in the next section. The ADC card has four input channels and two of them are used for the baseband signal input. It should also be noted that all transmit and receive ports that are used are DC blocked as the MMIC inputs and outputs are DC biased. The electronic boards and antennas are attached to an aluminum plate which can in turn be mounted on a tripod or turntable for field data collection. Interface signals between the radar front end and the PC (sampling clock, trigger, two baseband channels) are connected via 5 m long coaxial cables. The radar is powered from two lab bench supplies.

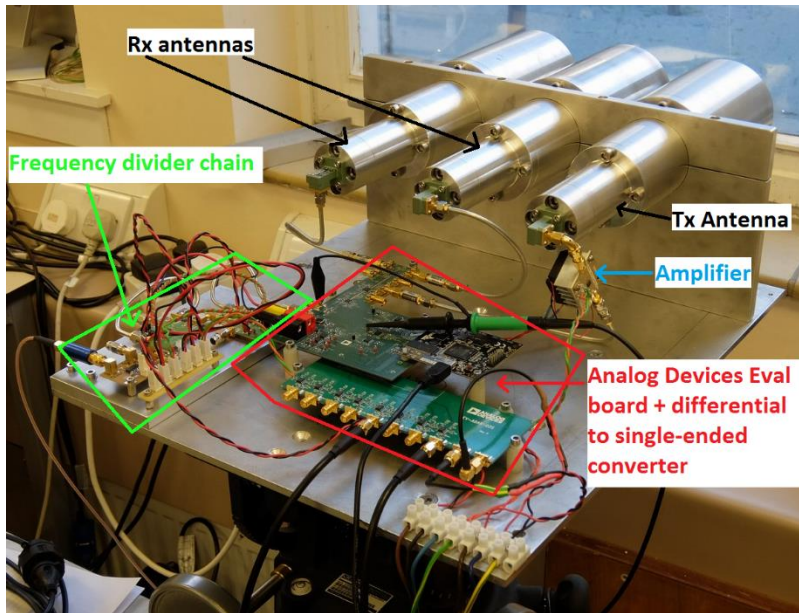


Figure 2. Physical configuration of the coherent 24 GHz radar system

### 3. HORN ANTENNA DESIGN

The primary purpose for the radar system was to be able to collect micro-Doppler signatures from small targets such as drones and birds (with radar cross sections of around  $-20$  dBsm) at around 150-200 m range. To meet this requirement, radar simulations suggested the required gain for the antennas should be around 25 dBi, which would also ensure a reasonably directional beam capable of isolating the target from clutter due to adjacent ground and trees. Low cost patch array antennas are available at 24 GHz but these have insufficient gain and quite wide beamwidths. Our solution was to design and build high gain horn antennas. Considering the gain, physical size and manufacturing complexity, a smooth-walled horn with a triple linear profile was designed, following the approach by Granet<sup>15</sup>, scaling a design which we had previously successfully manufactured at 94 GHz. The simulation was done by using the CORRUG mode matching software<sup>16</sup>. The 3 dB beamwidth is  $5.6^\circ$  in both E- and H-planes and the predicted gain is 24.56 dBi at 24 GHz. The antenna aperture diameter is 43.7 mm and the profile length is 297 mm. Three identical antennas were manufactured in four sections by directly machining aluminum. The three conical sections of the horn profile were turned on a lathe and the rectangular-to-circular transitions were machined by wire eroding. Commercial WR42 waveguide-to-coaxial adapters and semi-rigid coaxial cables are used to interface with the evaluation board.

The far field patterns of all three antennas were measured in the lab. Fig. 3 shows the antenna beam pattern plots for co-polar E-plane, co-polar H-plane and cross-polar D-plane at 24 GHz. The measured beam patterns agree very well with the simulations, validating the design and manufacturing process. Fig. 4 illustrates the simulated and measured directivity values over 18 to 26 GHz. It can be seen that the measured values agree with the simulations to within one dB. The measured gain at 24 GHz is 24.5 dBi. All the antennas were tested separately and yielded identical results. The two receive antennas are oriented to collect co- and cross-polar signals. The antenna mounting clamp enables arbitrary polarization to be configured by rotating the horns. By default we have set the transmit polarization to be horizontal.

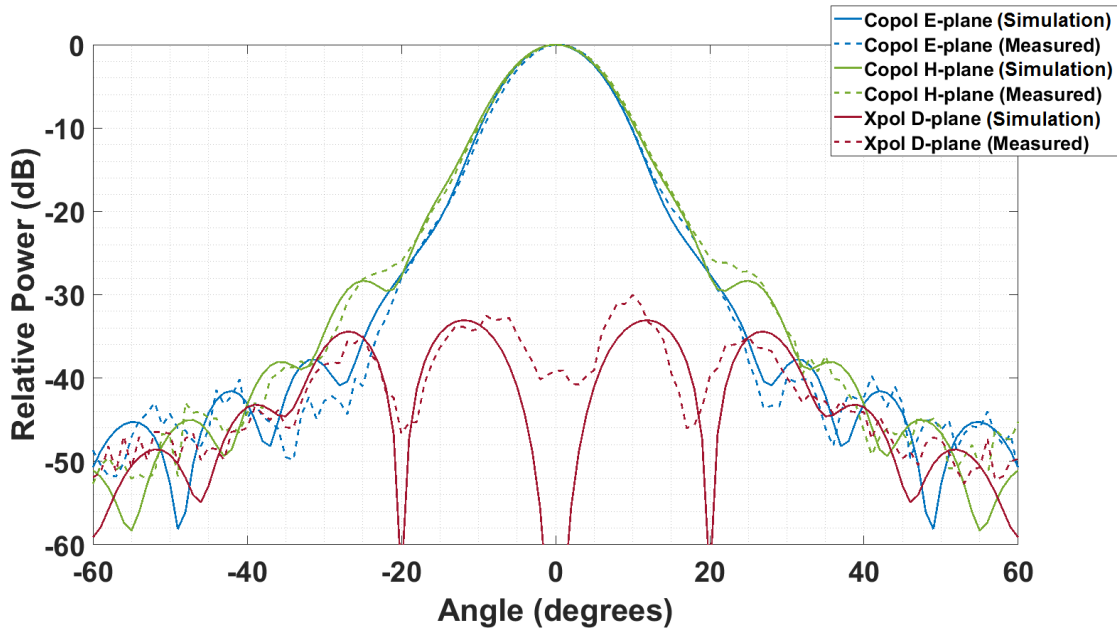


Figure 3. 24 GHz horn antenna beam pattern plots, both simulated and measured data

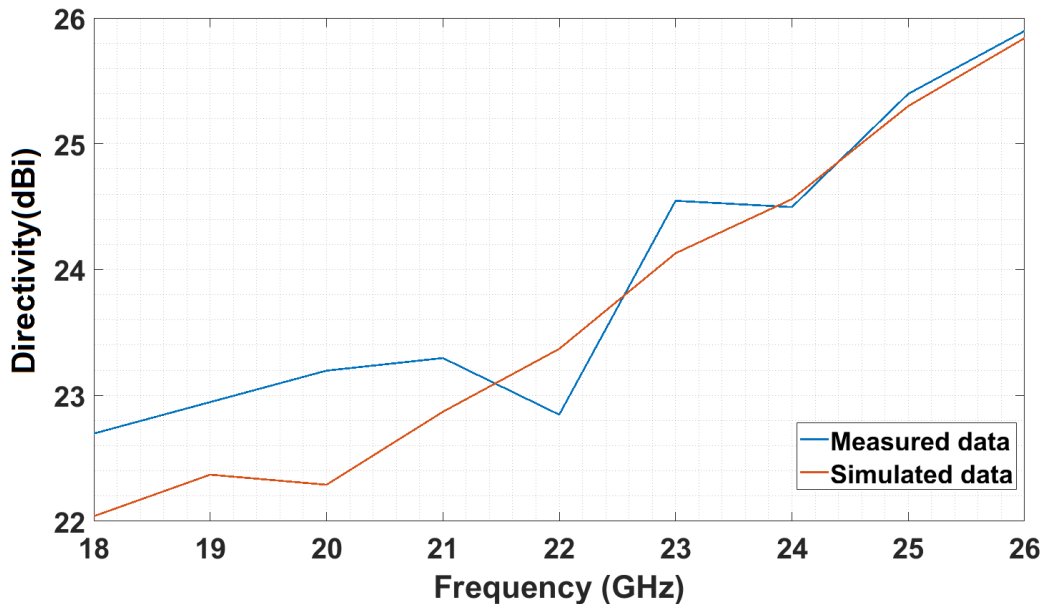


Figure 4. 24 GHz horn antenna directivity as a function of frequency, both simulated and measured data

#### 4. EXPERIMENTAL RESULTS AND MICRO-DOPPLER SIGNATURES

The radar system was calibrated using measured values of the total receiver gain and the amplifier gain and accounting for any cable loss or internal loss factors. A +8 dBsm trihedral mounted on a tripod was used for calibration measurements. Fig. 5 shows the calibration curve for the 24 GHz radar system, where the measured values agree well with the expected values within  $\pm 0.5$  dB. The measurement was not done beyond 94 m due to the ground clutter return from the longer ranges. The noise figure of the system has been verified as being  $\sim 10$  dB, set by the LNAs in the ADF5904. The ADC measurement is receiver noise limited rather than quantization noise limited and appears as a noise floor in the FFT of  $-77.5$  dBm. The predicted maximum range at which a  $-20$  dBsm target reaches 0 dB SNR is 315 m.

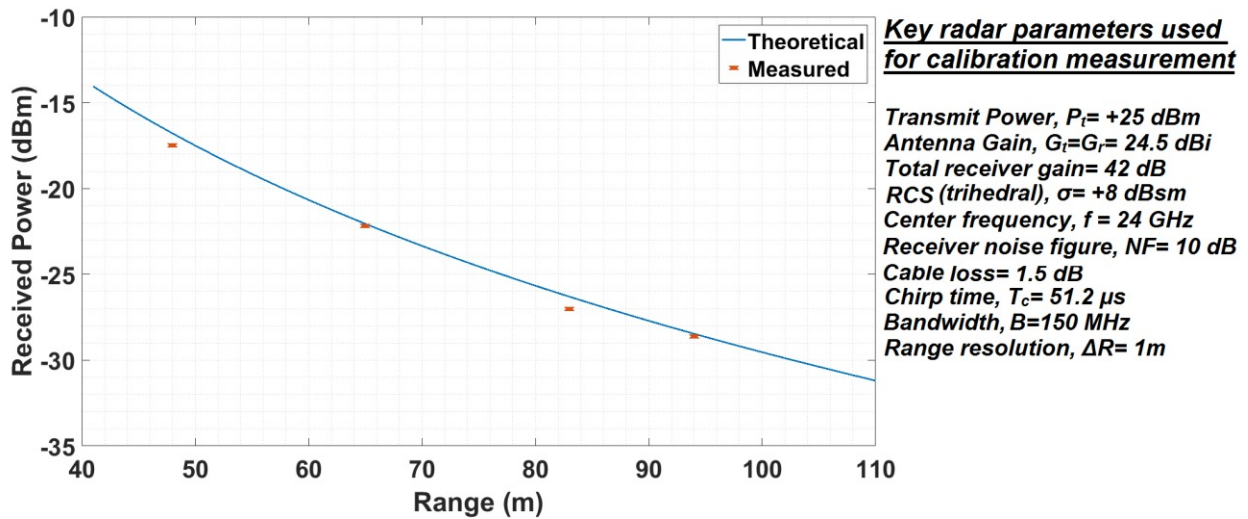


Figure 5. 24 GHz radar calibration curve for a +8 dBsm trihedral

The radar was used to obtain micro-Doppler signatures of three different targets: human, bird and drone. All these targets have intrinsically different micro-motion properties which would make the micro-Doppler signatures of each target unique. The radar parameter settings were chosen with regard to the expected Doppler values of the targets. The commercial drone used for the field trial (DJI Phantom 3 Standard) can reach bulk velocities up to around  $20 \text{ ms}^{-1}$ . During the trial, however, the drone is never flown at such high speed and the maximum bulk velocity is around  $10 \text{ ms}^{-1}$ . A similar maximum bulk velocity is expected from fast flying birds whilst that for an average human target will be lower.

It is harder to fully resolve the micro-Doppler from the very fast moving objects, such as the drone propeller blade rotation. The maximum unambiguous Doppler frequency for an FMCW radar is  $f_{d, \max} = 1/2t_s$ , where  $t_s$  is the chirp period. The maximum Doppler shift of a drone propeller blade can be readily calculated as  $((4\pi L\Omega)/\lambda) \cos\beta$ , where  $L$  is the length of the blade from its center,  $\Omega$  is the rotation rate in revolutions/second,  $\lambda$  is the radar wavelength and  $\beta$  is the elevation angle. Considering 100 Hz as the average drone propeller rotation rate and a blade length of 13 cm, a forward-looking 24 GHz radar will experience a maximum Doppler frequency of 13 kHz. To be fully sampled, this will require a 38  $\mu$ s chirp period. Such a fast chirp is very demanding for the ADF4159, also for the control code. Instead, the chirp period was chosen so that the bulk Doppler is fully resolved. The data collection was done with a chirp period of 234.8  $\mu$ s (actual chirp duration is 204.8  $\mu$ s and the delay between chirps is 30  $\mu$ s). The chirp repetition frequency (CRF) is then 4.25 kHz ( $\pm 2.125$  kHz maximum Doppler) giving a measurable velocity range of  $\pm 13.3 \text{ ms}^{-1}$ , where  $velocity = -(CRF * \lambda)/2$ . As 128 chirps are used for range-Doppler processing, the Doppler and velocity resolution values are then 33.25 kHz and  $0.2 \text{ ms}^{-1}$ , respectively. The sampling rate is set as 2.5 MHz, which gives 512 samples for each ramp and hence 256 range bins. It should be noted that the ratio of the sampling rate and the CRF should be an integer to avoid spurious Doppler signals. The chirp bandwidth was set to 150 MHz yielding 1 m range bins.

For better analysis of the micro-Doppler signatures of a target, spectrogram plots are produced offline in MATLAB. The processing is done using the conventional short time Fourier transform (STFT)<sup>3</sup> method. Fig. 6 shows the spectrogram plot of a human walking. The target was 25 m away from the radar. The strong zero-Doppler return is from the surrounding stationary clutter. The spectrogram enables one to visualize the various moving parts during walking. The movement of the arms, legs and torso can be observed from the spectrogram plot in Fig. 6.

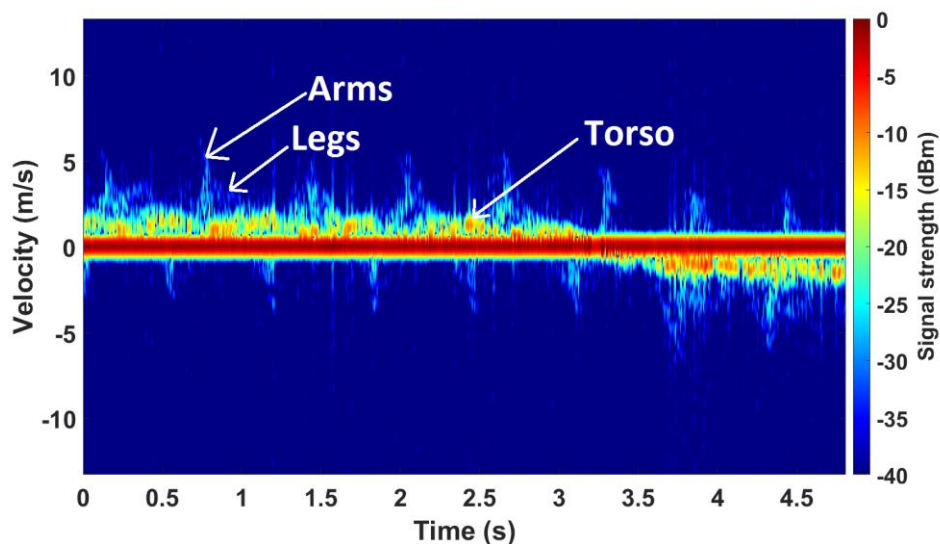


Figure 6. Spectrogram plot of a human walking 25 m away from the radar, revealing the micro-Doppler features

Fig. 7 shows the spectrogram plot of a Tawny Eagle flying. The bird was flying at 55 m range with a bulk velocity of around  $7 \text{ ms}^{-1}$ . The wing beats of the bird can be clearly seen. The wingbeat frequency and velocity (micro-Doppler) spread from the bulk-Doppler can also be calculated from the spectrogram, which are approximately 5 Hz and  $3 \text{ ms}^{-1}$  in this case.

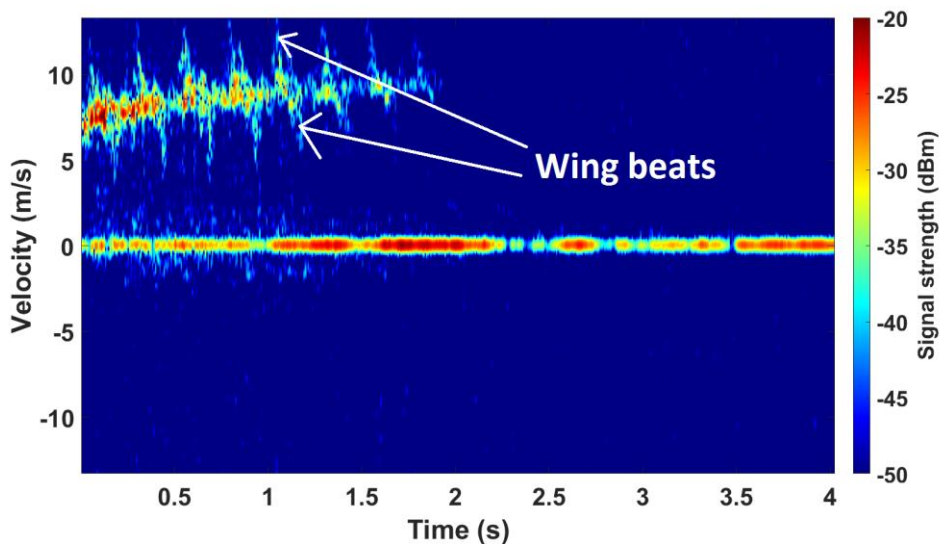


Figure 7. Spectrogram plot of a bird (Tawny Eagle) flying 55 m away from the radar, revealing the micro-Doppler features due to flapping wings

Fig. 8 illustrates the spectrogram plot of a commercial DJI Phantom 3 Standard which has a 4 propeller blades. The drone was flying 102.5 m away from the radar. As discussed earlier, the micro-Doppler return from the blades are aliased as the Doppler sampling rate is not high enough. Still, the micro-Doppler signature of the drone is very different from that of the bird or human. Helicopter Rotor Modulation (HERM) lines<sup>5</sup> are also observed in Fig. 8. Theoretically, the spacing of the HERM lines can be used to determine the propeller rotation rate if all the rotors have the same speed. In practice, that is not the case as they actually rotate at different speeds to maintain platform stability and orientation. So, the HERM line spacing is not constant due to the non-deterministic modulation of the signal returns from all the blades,

which can be observed in Fig. 8. Nonetheless, the presence of the HERM lines on the spectrogram is very valuable, which can later be used for target feature extraction.

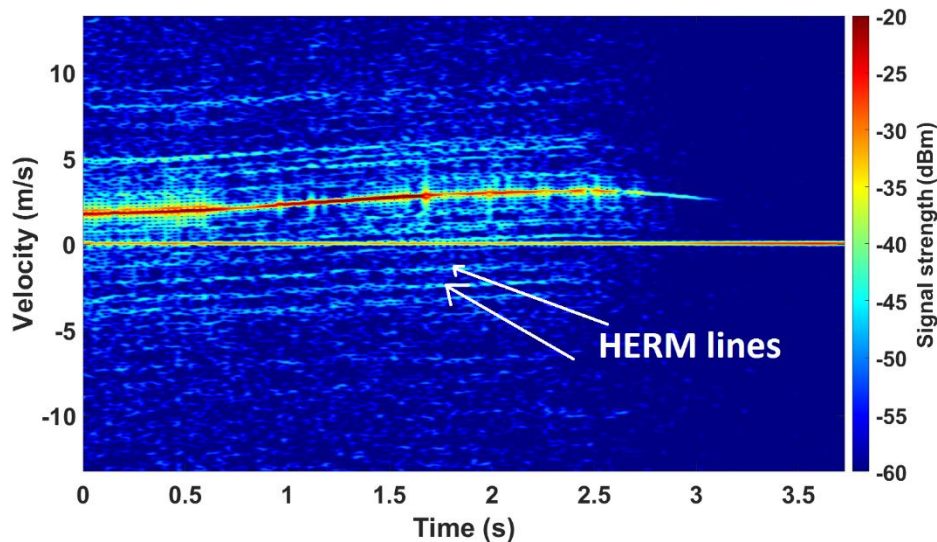


Figure 8. Spectrogram plot of a DJI Phantom 3 Standard, revealing the micro-Doppler features produced by the rotation of the four propeller blades

## 5. CONCLUSION AND FUTURE WORK

The main objective of this study was to build a 24 GHz radar system to be used for micro-Doppler signature collection from various targets. The design is based on a commercially available radar chipset evaluation board with modifications focused on ensuring that the radar is coherent and had sufficient range to measure small targets such as drones and birds at ranges of a few hundred meters. The radar hardware was built, tested and calibrated and integrated with real time control code written in C. Three identical smooth-walled triple-linear profile horn antennas were designed and built for the radar system. The radar has been used for data collection on various targets to collect micro-Doppler signatures at 24 GHz. We have presented example results for targets with three different types of micro-Doppler properties (human, bird, drone). The radar achieves a high level of performance and yields high fidelity data and can be used for different applications regarding target detection and classification by using micro-Doppler signatures.

This work has demonstrated the highly capable performance achievable with commercially available and relatively low cost 24 GHz chips. In the future, the intention is to further develop the system to make it more suited to field deployment as a surveillance radar. The current antenna performance is very satisfactory for data collection and demonstration purposes but high gain flat panel antennas would make the system more compact. Additionally, antennas with a narrow elevation fan beam, giving better angular resolution, would enable 360° surveillance with a motorized mount.

## 6. ACKNOWLEDGEMENTS

The authors acknowledge the funding received from the Science and Technology Facilities Council which has supported this work under grant ST/N006569/1. The authors acknowledge and thank Dr Graham Smith and Dr Robert I. Hunter for helping with the antenna design and CAD modelling. Finally, the authors also thank Elite Falconry, Kirkcaldy, Scotland, for flying the birds.

## REFERENCES

- [1] Chen, V. C., Li, F., Ho, S. S. and Wechsler, H., "Micro-doppler effect in radar: Phenomenon, model, and simulation study," *IEEE Trans. Aerosp. Electron. Syst.* **42**(1), 2–21 (2006).
- [2] Chen, V. C., [The micro-doppler effect in radar], Artech House (2011).

- [3] Chen, V. C. and Shie Qian., “Joint time-frequency transform for radar range-Doppler imaging,” *IEEE Trans. Aerosp. Electron. Syst.* **34**(2), 486–499 (1998).
- [4] Thayaparan, T., Abrol, S., Riseborough, E., Stankovic, L., Lamothe, D. and Duff, G., “Analysis of radar micro-Doppler signatures from experimental helicopter and human data,” *IET Radar, Sonar Navig.* **1**(4), 289 (2007).
- [5] Wit, J. de., “Micro-Doppler analysis of small UAVs,” 2012 9th Eur. Radar Conf. 31 Oct. - 2 Novemb. 2012, Amsterdam, Netherlands, 210–213 (2012).
- [6] Tahmouh, D., “Detection of small UAV helicopters using micro-Doppler,” *Proc. SPIE 9077, Radar Sens. Technol. XVIII 9077*, K. I. Ranney and A. Doerry, Eds., 907717, International Society for Optics and Photonics (2014).
- [7] Molchanov, P., Harmanny, R. I. A., de Wit, J. J. M., Egiazarian, K. and Astola, J., “Classification of small UAVs and birds by micro-Doppler signatures,” *Int. J. Microw. Wirel. Technol.* **6**(3–4), 435–444 (2014).
- [8] Ritchie, M., Fioranelli, F., Borrion, H. and Griffiths, H., “Classification of loaded/unloaded micro-drones using multistatic radar,” *Electron. Lett.* **51**(22), 1813–1815 (2015).
- [9] Ritchie, M., Fioranelli, F., Griffiths, H. and Torvik, B., “Monostatic and bistatic radar measurements of birds and micro-drone,” 2016 IEEE Radar Conf., 1–5, IEEE (2016).
- [10] Bjorklund, S., Petersson, H., Nezirovic, A., et al., “Millimeter-wave radar micro-Doppler signatures of human motion,” *Int. Radar Symp. IRS 2011*, DCM Druck Center, Leipzig (2011).
- [11] Robertson, D. A. and Cassidy, S. L., “Micro-doppler and vibrometry at millimeter and sub-millimeter wavelengths,” *Proc. SPIE 8714, Radar Sens. Technol. XVII 8714*, K. I. Ranney and A. Doerry, Eds., 87141C, International Society for Optics and Photonics (2013).
- [12] Robertson, D. A., Brooker, G. M. and Beasley, P. D. L., “Very low-phase noise, coherent 94GHz radar for micro-Doppler and vibrometry studies,” *Proc. SPIE 9077, Radar Sens. Technol. XVIII 9077*, K. I. Ranney and A. Doerry, Eds., 907719, International Society for Optics and Photonics (2014).
- [13] Rahman, S. and Robertson, D. A., “Millimeter-wave micro-Doppler measurements of small UAVs,” *Proc. SPIE 10188, Radar Sens. Technol. XXI 10188*, K. I. Ranney and A. Doerry, Eds., 101880T, International Society for Optics and Photonics (2017).
- [14] “EVAL-RADAR-MMIC Evaluation Board | Analog Devices.”, <<http://www.analog.com/en/design-center/evaluation-hardware-and-software/evaluation-boards-kits/eval-radar-mmic.html#eb-overview>> (8 March 2018 ).
- [15] Granet, C., James, G. L., Bolton, R. and Moorey, G., “A Smooth-Walled Spline-Profile Horn as an Alternative to the Corrugated Horn for Wide Band Millimeter-Wave Applications,” *IEEE Trans. Antennas Propag.* **52**(3), 848–854 (2004).
- [16] “CORRUG, SMT Consultancies Ltd Home.”, <<http://www.smtconsultancies.co.uk/products/corrug/corrug.php>> (19 March 2018 ).